Steel and Composite Structures, *Vol. 19, No. 1 (2015) 173-190*
DOI: http://dx.doi.org/10.12989/scs.2015.19.1.173

Fragility assessment of buckling-restrained braced frames under near-field earthquakes

Ahmad F. Ghowsi and Dipti R. Sahoo *

Department of Civil Engineering, Indian Institute of Technology Delhi, New Delhi-110016, India

(*Received April 13, 2014, Revised November 01, 2014, Accepted December 30, 2014*)

Abstract. This study presents an analytical investigation on the seismic response of a medium-rise buckling-restrained braced frame (BRBF) under the near-fault ground motions. A seven-story BRBF is designed as per the current code provisions for five different combinations of brace configurations and beam-column connections. Two types of brace configurations (i.e., Chevron and Double-X) are considered along with a combination of the moment-resisting and the non-moment-resisting beam-to-column connections for the study frame. Nonlinear dynamic analyses are carried out for all study frames for an ensemble of forty SAC near-fault ground motions. The main parameters evaluated are the interstory and residual drift response, brace displacement ductility, and plastic hinge mechanisms. Fragility curves are developed using log-normal probability density functions for all study frames considering the interstory drift ratio and residual drift ratio as the damage parameters. The average interstory drift response of BRBFs with Double-X brace configurations significantly exceeded the allowable drift limit of 2%. The maximum displacement ductility characteristics of BRBs is efficiently utilized under the seismic loading if these braces are arranged in the Double-X configurations instead of Chevron configurations in BRBFs located in the near-fault regions. However, BRBFs with the Double-X brace configurations exhibit the higher interstory drift and residual drift response under near-fault ground motions due to the formation of plastic hinges in the columns and beams at the intermediate story levels.

Keywords: buckling-restrained braces; fragility curves; near-fault regions; seismic analysis; steel frames

1. Introduction

Buckling-restrained braced frames (BRBFs) are considered as one of the efficient lateral force-resisting systems in buildings located in the high-seismic areas due to excellent energy dissipation and nearly-equal load carrying capacity of buckling-restrained braces (BRBs). Fig. 1(a) shows the schematic representation of various segments of a BRB. The core segment of a BRB is filled with unbonded concrete (mortar) that offers resistance to both in-plane and out-of-plane buckling of the steel plate inside, thereby increasing the axial resistance and energy dissipation potential of BRBs under the compressive axial loading. A number of tests at the component level

*Corresponding author, Assistant Professor, Ph.D., E-mail: drsahoo@civil.iitd.ac.in
[a] Ph.D. Student, E-mail: faieq.ghowsi@gmail.com

http://www.techno-press.org/?journal=scs&subpage=8 ISSN: 1229-9367 (Print), 1598-6233 (Online)

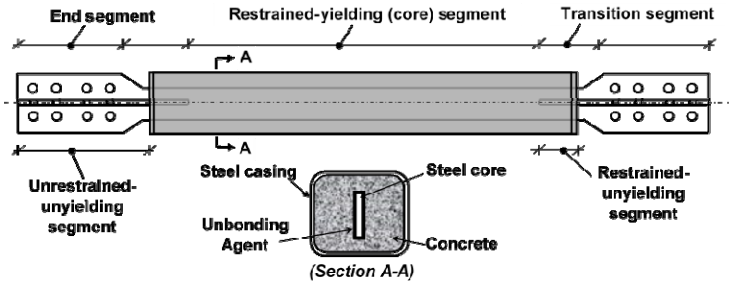

(a)

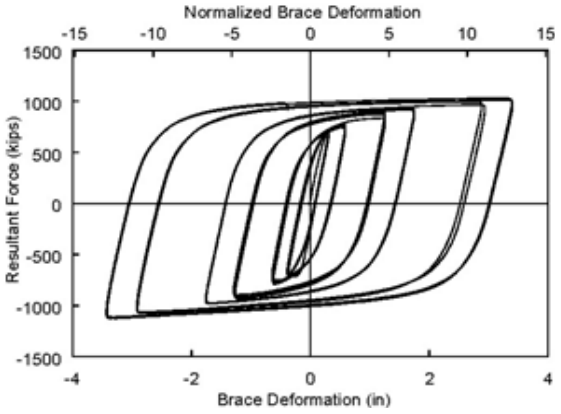

(b)

Fig. 1 Typical (a) cross-section; and (b) hysteretic response of a BRB

as well as the system level of BRBFs have been conducted by various researchers to investigate their seismic performance (e.g., Watanabe *et al*. 1988, Aiken *et al*. 2002, Iwata *et al*. 2003, Merritt *et al*. 2003, Romero *et al*. 2003, Tsai *et al*. 2003a, Black *et al*. 2004, Fahnestock *et al*. 2007, Chou *et al*. 2012). Fig. 1(b) shows a typical hysteretic response of BRBs under cyclic loading condition (Merritt *et al*. 2003). The main parameters studied in these tests are the displacement ductility and cumulative displacement ductility, the energy dissipation potential, the compressive over-strength factors, the strain-hardening factors, and the performance of frames members by varying the core cross-sections, the detailing of non-yielding segments and the end connections of BRBs.

Apart from the detailing of end connections, the type of beam-to-column connections and the arrangement of BRBs largely influence the seismic response of BRBFs (Field and Ko 2004, Lin *et al*. 2005, Fahnestock *et al*. 2007, Ghowsi and Sahoo 2013). Usually, the beam-to-column connections in a steel braced frame can be of moment-resisting (rigid) or non-moment-resisting (pinned) types. Usually, two types of BRB configurations, namely, Chevron (Inverted-V) and Double-story-X are commonly used in BRBFs. Ghowsi and Sahoo (2013) concluded that Double-story-X configuration of BRBs resulted in the relatively larger post-earthquake residual drift response of BRBFs as compared to those in Chevron configurations under the far-field earthquakes. Further, although the pinned beam-to-column connections resulted in the smaller interstory drift response of BRBFs as compared to the rigid connections, plastic hinging in the intermediate columns may induce the soft-story collapse. While the extensive studies have been

carried out on the seismic response of BRBFs under the far-field earthquakes, research on their performance under the near-field earthquakes is rather limited (e.g., Baghbanijavid *et al*. 2010, Shakib and Safi 2012, Avci-Karatas *et al*. 2013). The near-fault ground motions often contain strong dynamic long period pulses that may lead to the permanent ground displacements. The effect of this type of ground motions are still not known and hence, are not included in the design spectrums of various international codes. The past studies have shown that the near-fault ground motions can cause extensive structural damages as compared to the far-fault ground motions. Significant post-earthquake residual drift response can be expected in BRBFs, which may affect the performance of non-structural systems (Baghbanijavid *et al*. 2010). Hence, there is a need of further study to investigate the response of BRBFs under the near-fault ground motions.

In this study, an analytical investigation has been conducted on a medium-rise (seven-story) BRBF system. Both Chevron and Double-story-X brace configurations are considered in combination with either rigid or pinned beam-to-column connections. Seismic performance of all these study frames is evaluated through nonlinear dynamic (time-history) analysis for an ensemble of forty near-field ground motions derived from the historical records and the physical simulation. The main parameters studied are the interstory drift response, residual drift response, hinge mechanism, and maximum brace ductility demand. Fragility analyses are carried out to investigate the probability of exceeding a particular damage state at a specified hazard level. The main objectives of this study are: (a) to evaluate the seismic response of a BRBF designed based on the code provisions under near-fault ground motions; (b) to investigate the effect of the beam-to-column connections and the BRB configurations on the overall seismic response of BRBFs; and (c) to carry out the fragility assessment of the BRBFs considering the interstory and residual drift ratio as the damage indicators.

2. Details of study building

A seven-story building of plan dimension of 36.60 m × 22.87 m and 25.33 m high, as shown in Fig. 2(a), is considered as the study building in which there are five bays along the longer direction and three bays along the shorter direction. The height of each story is 3.51 m except the first story of 4.27 m in height. All perimeter braced bays are symmetrically located in the building plan. All interior frames are the gravity-load resisting frames. Braced frame (BF-2) along the shorter direction of the building plan, as shown in the Fig. 2(b), is considered as the study frame in which BRBs are placed in all the story levels. López and Sabelli (2004) have previously designed the same building with BRBs arranged in Chevron configuration with all rigid beam-to-column connections. Total seismic weight of the building is estimated as 26.38 MN. Using the spectral acceleration values S_{DS} and S_{D1} as 1.03 g and 0.89 g, respectively, the design base shear for the building is found to be 12.8% of the seismic weight. The approximate and the allowable maximum values of fundamental period of the building are estimated as 0.82 sec. as per ASCE/SEI 7-10 (2010) provisions using a C_u value of 1.4. Modal analysis results showed that the fundamental period of the BRBF considered in this study is about 1.10 sec. Table 1 summarizes the design drift values at various floor levels of the BRBF (BF-2). Design drift values are computed from the elastic drift values using a deflection amplification factor (C_d) equal to 5.0 (FEMA 450 2003). It is worth mentioning that the allowable drift ratio is considered as 2.0% as per ASCE/SEI 7-10 (2010) provisions.

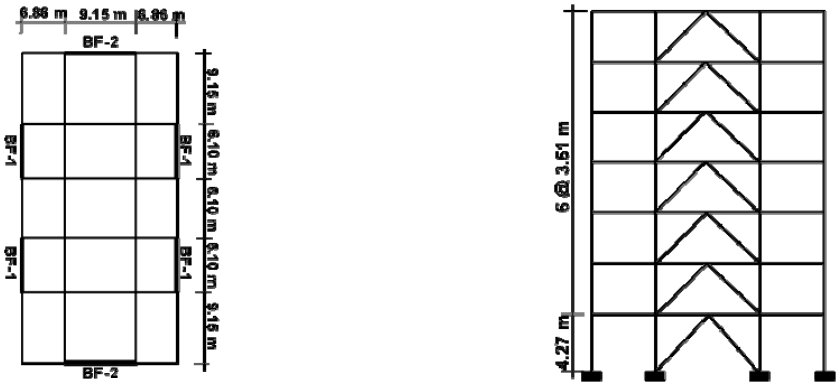

(a) (b)

Fig. 2 (a) Plan; and (b) elevation views of the study building

Table 1 Design story drifts for BF-2 frame computed as per current code provisions

Story	h (m)	Δ_x (cm)	Δ (cm)	Δ_a (cm)	θ_x (%)	θ_M (%)	θ_a (%)
7th	3.51	1.30	6.45	7.01	0.37	1.84	2.00
6th	3.51	1.27	6.35	7.01	0.36	1.81	2.00
5th	3.51	1.12	5.61	7.01	0.32	1.60	2.00
4th	3.51	1.02	5.08	7.01	0.29	1.45	2.00
3rd	3.51	0.97	4.88	7.01	0.28	1.39	2.00
2nd	3.51	0.76	3.76	7.01	0.21	1.07	2.00
1st	4.27	0.69	3.38	8.53	0.16	0.79	2.00

*Note: h = Story height; Δ_x = Elastic story drift; Δ = Design story drift; Δ_a = Allowable story drift; θ_x = Interstory drift; θ_M = Design drift ratio; θ_a = Allowable drift ratio

Five design cases of BRBFs with the BRBs arranged in either Chevron or Double-X configurations along with the moment-resisting or non-moment-resisting beam-to-column connections are investigated in this study. These are: (a) CRBC frame with Chevron BRBs and all rigid beam-column (RBC) connections; (b) CPBC frame with Chevron BRBs and all pinned beam-to-column (PBC) connections; (c) XRBC frame with Double-X braces and all RBC connections; (d) XPBC frame with Double-X braces and all PBC connections; and (e) XAPBC frame with Double-X braces and alternate RBC and PBC connections. Fig. 3 shows the details of design cases considered in this study and the sections used as beams and columns. In case of XAPBC frame, the RBC connections are used at the beam-column connections where the BRBs are present; otherwise, the PBC connections are used. BRB sizes along the frame height are determined based on the assumption that the design story shear is proportionally divided into the braces and the braced frame columns depending on their relative rigidity (SEAOC 1999). Linear elastic analysis is carried out to estimate the axial force in the braces for various load combinations using the applicable load factors. BRB sections are chosen such that ratio of the maximum axial force demand to the yield resistance of BRBs is less than or equal to unity. As followed in the practice, the core areas of BRBs used in this study are rounded off to a nearest 0.5 in^2 (322.6 mm^2)

value. In all cases, the pinned connections are assumed between the BRBs and frame members. The value of response reduction factor (R) is used as 8 in calculating the design base shear for the BRBF with either PBC or RBC connections as per ASCE/SEI 7-10 (2010) provisions. Tensile yield stress of BRB material is considered as 345 MPa. The value of material overstrength factor (R_y) is considered as 1.0. Compression overstrength (β) and strain-hardening (ω) factors of BRBs are assumed as 1.1 and 1.3, respectively (Sahoo and Chao 2010). Table 2 summarizes the properties of BRBs used at various story levels of the study frames. W16×50 is used as beams at all floor levels, whereas W14×211, W14×145 and W14×75 sections are used as columns at 1st-2nd, 3rd-4th, and 5th-7th story levels of the study frames, respectively (Fig. 3). The width-to-thickness (b/t) ratio of flanges of sections used as beams and columns is smaller than $0.3\sqrt{(E/F_y)}$; whereas the depth-to-thickness (h/t) ratio of webs of sections is less than $1.49\sqrt{(E/F_y)}$ as per ANSI/AISC 341-10 (2010) provisions. The values of Young's modulus (E) and material yield stress (F_y) are considered as 200 GPa and 345 MPa, respectively. The effect of axial load on the compression webs of column section has also been considered in computing the limiting value of h/t ratio.

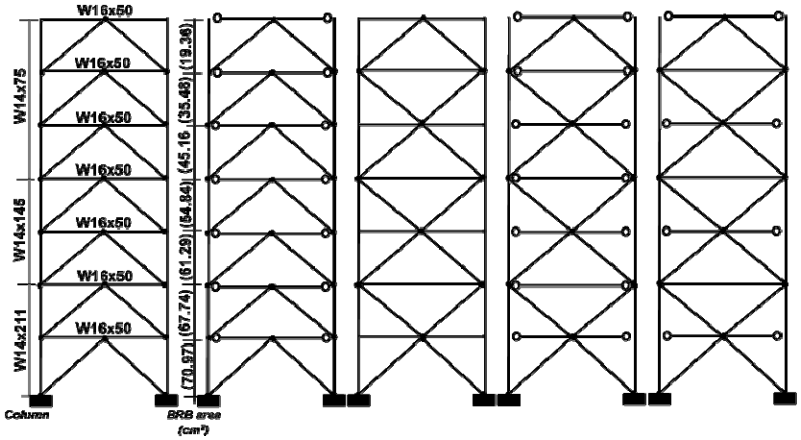

(a) (b) (c) (d) (e)

Fig. 3 Details of study frames (a) CRBC; (b) CPBC; (C) XRBC; (d) XPBC; (e) XAPBC (*Note*: CRBC frame has been earlier studied by López and Sabelli 2004)

Table 2 Geometric properties of BRBs used at various floor levels

Story	a (mm^2)	F (kN)		K (kN/mm)	$\delta = F/K$ (mm)	
		Tension	Comp.		Tension	Comp.
1	7096.8	2446.5	2691.2	324.4	7.54	8.30
2	6774.2	2335.3	2566.6	335.9	6.95	7.65
3	6129.0	2112.9	2324.2	303.8	6.95	7.65
4	5483.9	1890.5	2077.3	272.0	6.95	7.65
5	4516.1	1556.9	1712.6	206.5	6.95	7.65
6	3548.4	1223.3	1345.6	51.8	6.95	7.65
7	1935.5	667.2	734.0	88.4	6.95	7.65

3. Analytical modeling

Two-dimensional models of the study frames are analyzed using a computer package SAP 2000 (CSI 2009). All members are modeled as the frame elements with proper boundary conditions. Columns at the first story level of the BRBFs are assumed to be fixed at their bases. The tributary floor mass at each floor level has been included in the analytical models. *P-Delta* effect due to gravity loads on the frames is considered by modeling of a single leaning (gravity) column pinned at its base. The leaning column is constrained to have the same lateral displacement as the adjacent braced frame column at each floor level by using the pinned rigid link beams connecting the braced frame columns and the leaning column. All gravity loads are applied at the respective nodes along the height of the leaning column. Nonlinear behavior of the frame members is modeled by assigning the lumped plastic hinges at the potential locations. Fig. 4 shows the plastic hinge properties used for the modeling of inelastic properties of BRBs and frame members in which the generalized force and displacement values are normalized with respect to their corresponding yield values. Nonlinear axial force-displacement behavior of BRBs is modeled by assigning (axial) plastic hinges at their mid-lengths. The axial elastic stiffness of BRBs is estimated using the area of core segments and the length of core segment equal to 70% of the total length. It may be noted that the effective axial elastic stiffness of a BRB should consider the stiffness contribution from the end segments and the transition segments in addition to the core segment. This can be estimated by using a mathematical model consisting of three elastic spring elements connected in series, each representing the end, transition, and core segments of BRBs (Huang and Tsai 2002). Though the value of effective axial elastic stiffness of BRBs is usually smaller than the elastic stiffness of core segments, this effect should not have a major influence on the estimation of drift response BRBFs using nonlinear analysis. The post-yield stiffness of BRBs is assumed as 2% of their elastic (core) stiffness.

The yield displacements of BRBs at different floor levels are summarized in Table 2. Past studies showed that the BRBs are capable of exhibiting the deformation ductility greater than 20 (e.g., Usami *et al*. 2003, Tsai *et al*. 2003a). This can be achieved by adopting proper detailing scheme, which primarily involves the specification of proper internal clearance between the

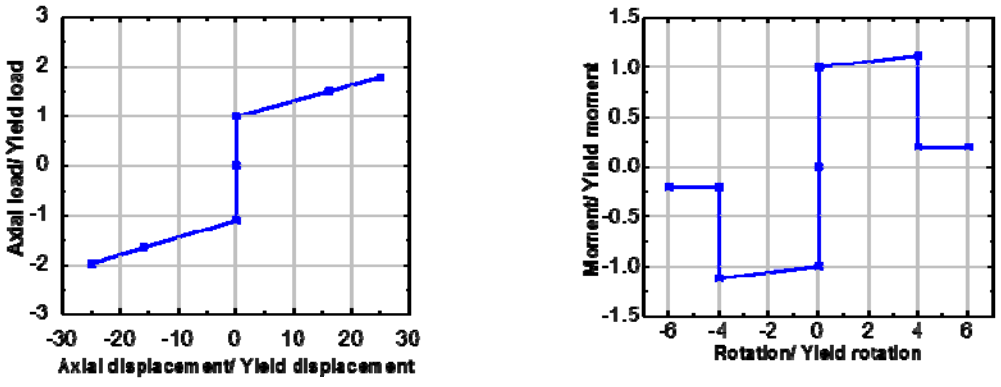

(a) (b)

Fig. 4 Normalized inelastic: (a) force-deformation behavior of BRB; and (b) moment-rotation behavior of frame members used in the analytical modelling

surface of core segment and the confining concrete (Fahnestock *et al*. 2007). Hence, a ductility value of 25 considered in the analytical models in this study represent a maximum value prior to the brace fracture. Lumped plastic hinges are assigned at both ends of columns and beams (only with RBC connections). The moment-rotation (M-θ) response is considered at the plastic hinges. Various parameters of the moment-rotation plastic hinges have been adopted from FEMA 356 (2000) provisions as shown in Fig. 4(b). Since the presence of axial load reduces the plastic moment capacity of columns, axial force-bending moment (P-M) interaction behavior (FEMA 356 2000) provisions is considered at the plastic hinges in columns. Kinematic hardening is considered in the hysteretic behavior of all members. Rigid end zones at the beam-column connections and the beam segment between the column face and the pinned connection location are not explicitly modeled in this study. Linear modal analysis results showed that there is no significant difference in the fundamental period values by using different brace configurations and beam-column connections in the study frames.

4. Selection of ground motions

Nonlinear dynamic analyses are carried out for all study frames for a set of twenty two-component near-fault time-history ground motions developed by Somerville *et al*. (1997) for SAC projects. The first suite of ten two-component (NF01-20) acceleration time-histories are derived from the historical recordings, whereas the second set of ten two-component (NF21-40) time-histories are developed from the physical simulations of fault rupture and seismic wave propagation through soil strata. The individual components of each ground motion is rotated 45 degrees away from the fault-normal and fault-parallel orientations. These forty ground motions represent different fault mechanisms in the magnitude range of 6.75 to 7.5 with a source-to-site distance varying from 0-18 km. These ground motions form a set that provides a reasonable representation of the median and variability of the ground motions that a given site may experience from a nearby earthquake of magnitude 7.0 at a distance about 5 km. This magnitude-distance pair controls the 10% in 50-year ground motions in many regions of California, USA (Somerville *et al*. 1997). Fig. 5(a) shows the

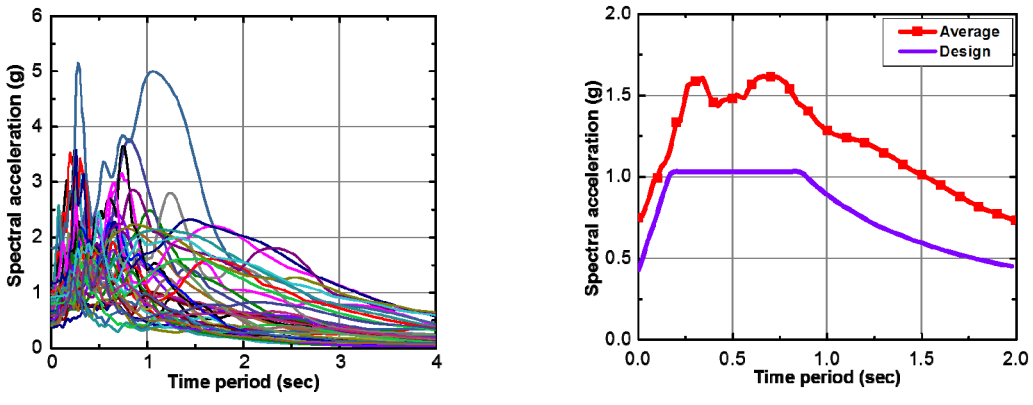

(a) (b)

Fig. 5 (a) Response spectra of all selected ground motions; and (b) comparison of average response spectra with the design spectrum used in this study

response spectra of all the selected near-fault ground motions selected in this study. As expected, these ground motions contains pulse-like and long-period spectral accelerations. The maximum value of spectral acceleration is noted for NF23 ground motion near the time period of 1.0 sec. A comparison of the average response spectra with the design spectrum considered in this study is shown in Fig. 5(b). Although no scale factors are applied on these ground motions, the average response spectra is well above the design spectrum by a margin of 40% in the period range of 0.5-1.5 sec.

5. Analysis results

As stated earlier, nonlinear time-history analyses are carried out for all the design cases under forty near-field ground motions. The main parameters investigated are interstory drift ratio (ISDR), residual drift ratio (RDR), state of damages in frame members, BRB hysteretic response and displacement ductility behavior. Drift ratio is defined as the ratio of story displacement to the corresponding story height. For the drift response, various statistical quantities, such as, mean (μ), standard deviation (σ), etc. are evaluated for all design cases under the selected ground motions. It worth mentioning that ISDR response is considered as an indicator of damages in a structure.

5.1 Interstory drift response

Fig. 6(a) shows the displacement response at the second story level of BRBFs under NF31 ground motion. All BRBFs exhibited similar displacement-time response. At about 17 sec. of ground motion, a sharp jump in the displacement response of amplitude 400 mm is noticed at the second floor level. Beyond this time instance, the displacement response of BRBFs oscillated at a shifted position of 100 mm displacement amplitude level showing a residual displacement till the end of the earthquake. Fig. 6(b) shows the axial load–displacement (i.e., hysteretic) response of BRB at the first story level of BRBFs. The linear elastic behavior of BRB is noted initially till the yielding point beyond which the origin of the hysteretic response shifted to a displacement level of

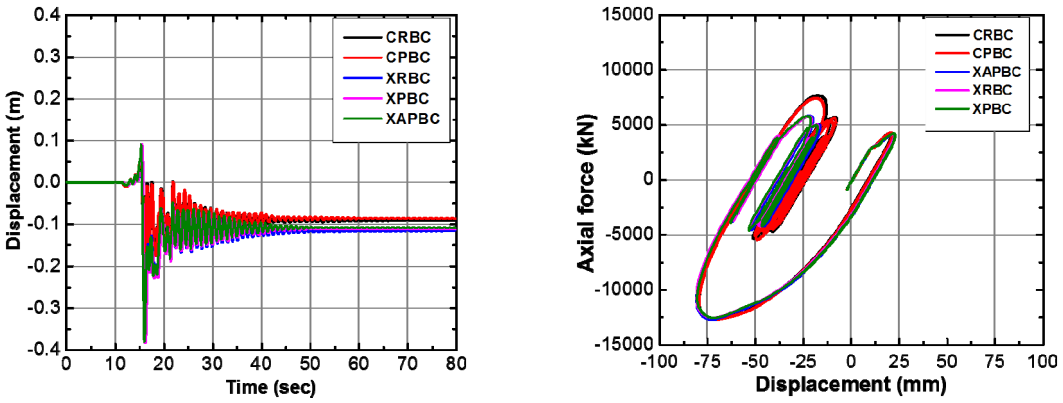

(a) (b)

Fig. 6 (a) Displacement-time history; and (b) hysteretic response of BRBs under NF31 ground motion

25 mm at which the BRBs continued to dissipate the hysteretic energy. The maximum value of BRB displacement is noted as 80 mm under compression loading.

Fig. 7(a) shows the peak ISDR response of BRBFs under the selected forty ground motions. The μ and ($\mu + \sigma$) values of drift response are also shown in the figure. The distribution of mean ISDR response is uniform along the height of the BRBFs with Chevron braces, whereas a relatively higher value of ISDR is noted at the story level where the braces are connected at the mid-pints of beams in case of the BRBFs with Double-X brace configurations. The μ and ($\mu + \sigma$) values of ISDR are noted as about 2% and 3%, respectively, for BRBFs with the Chevron braces. The absolute maximum ISDR response exceeded a value of 5% under some ground motions. In case of Double-X brace configurations, the μ and ($\mu + \sigma$) values of ISDR are noted as about 2.5% and 4.0%, respectively, with the absolute maximum ISDR value exceeding 6.5% drift level under some ground motions. No significant difference in the peak ISDR response is noted between the RBC and PBC connections. Table 3 summarizes the mean values of ISDR at various story levels of BRBFs with Chevron as well as Double-X brace configurations. The maximum value of average ISDR response is noted at the fourth story level of BRBFs. Except the seventh story level, the mean value of ISDR response exceeded the design values at all the story levels of BRBFs (Table 3). While the average values of ISDR response for BRBFs with Chevron BRB configurations were less than the allowable drift limit of 2%, the ISDR values for the BRBFs with Double-X configurations exceed this allowable limit at the story levels where braces did not intercept the beams.

Table 3 Comparison of average values of peak ISDR response of BRBFs with design values

Story	CRBC		CPBC		XRBC		XPBC		XAPBC		Design value
	μ	$\mu+\sigma$	μ	$\mu+\sigma$	μ	$\mu+\sigma$	μ	$\mu+\sigma$	μ	$\mu+\sigma$	
7	1.71	2.44	1.75	2.57	1.46	2.09	1.59	2.27	1.53	2.18	1.84
6	1.86	2.71	1.84	2.76	2.17	3.33	2.28	3.50	2.24	3.42	1.81
5	1.96	2.93	1.93	2.96	1.60	2.53	1.64	2.55	1.64	2.55	1.60
4	1.95	2.99	1.93	3.02	2.50	4.22	2.56	4.31	2.52	4.22	1.45
3	1.94	3.00	1.90	3.01	1.56	2.58	1.58	2.59	1.58	2.60	1.39
2	1.91	2.99	1.88	3.01	2.35	4.08	2.39	4.12	2.37	4.09	1.07
1	1.67	2.67	1.62	2.64	1.25	2.14	1.25	2.11	1.27	2.14	0.79

Table 4 Statistical values of RDR response of BRBFs

Story	CRBC		CPBC		XRBC		XPBC		XAPBC	
	μ	$\mu+\sigma$	μ	$\mu+\sigma$	μ	$\mu+\sigma$	μ	$\mu+\sigma$	μ	$\mu+\sigma$
7	0.19	0.35	0.24	0.48	0.27	0.57	0.39	0.84	0.32	0.70
6	0.23	0.42	0.26	0.50	0.34	0.71	0.43	0.93	0.36	0.81
5	0.25	0.48	0.26	0.53	0.35	0.80	0.40	0.91	0.37	0.86
4	0.26	0.51	0.27	0.54	0.42	0.96	0.46	1.06	0.42	0.96
3	0.26	0.54	0.26	0.55	0.38	0.87	0.40	0.93	0.38	0.90
2	0.26	0.57	0.26	0.56	0.42	0.98	0.45	1.04	0.42	0.98
1	0.27	0.59	0.25	0.56	0.32	0.77	0.32	0.77	0.32	0.76

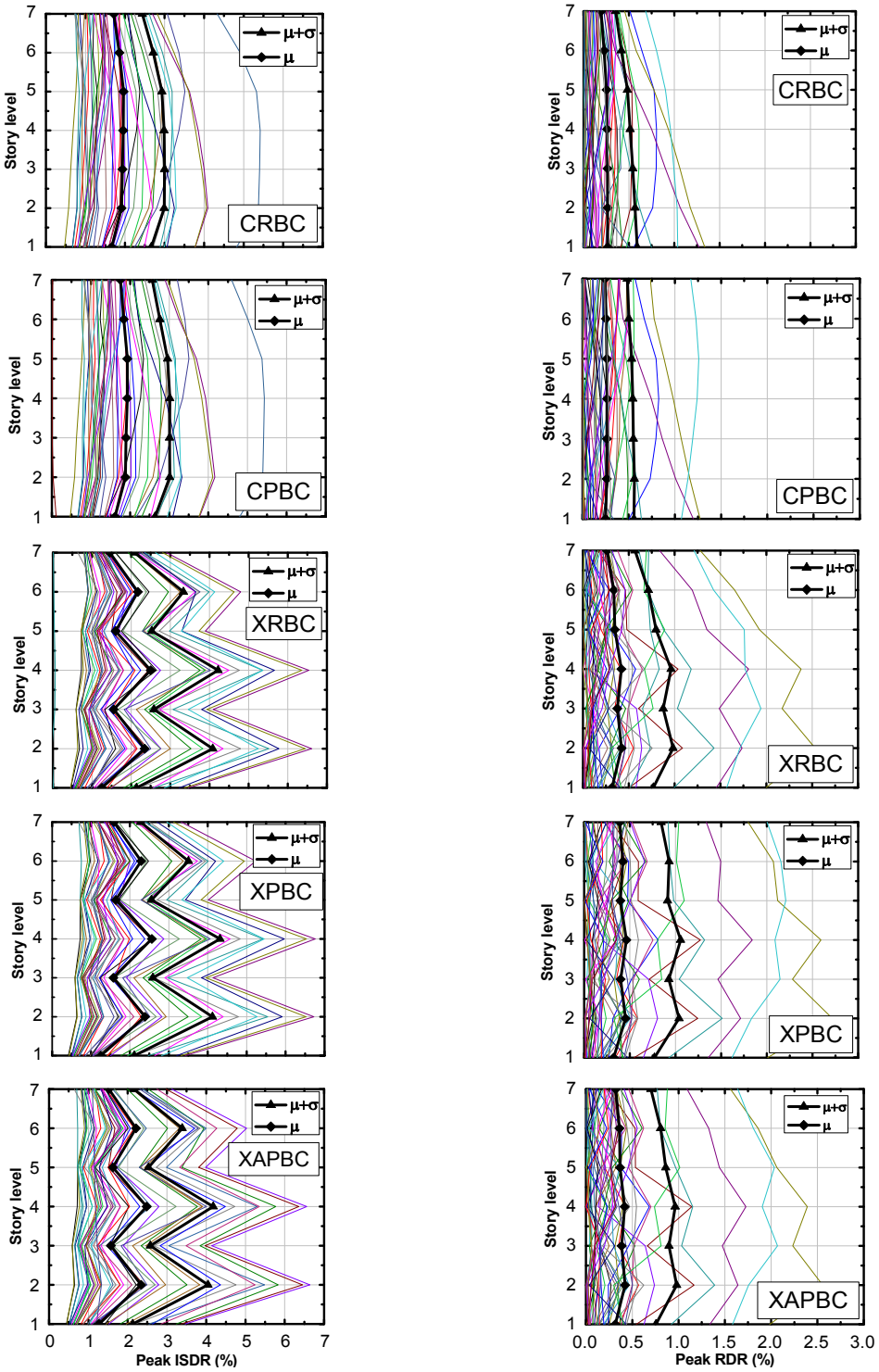

Fig. 7 (a) ISDR; and (b) RDR response of BRBFs under all selected ground motions

5.2 Residual drift response

Fig. 7(b) shows the peak RDR response at various story levels of the BRBFs under the selected ground motions. Unlike ISDR response, the distribution of the RDR response is found to be uniform over the height of BRBFs with Double-X BRB configurations. The μ and $(\mu + \sigma)$ values of RDR are found to be about 0.2% and 0.6%, respectively, for BRBFs with the Chevron brace configurations. The absolute maximum RDR response is found to be close to 1.4% under some ground motions. In case of Double-X brace configurations, the μ and $(\mu + \sigma)$ values of RDR are about 0.5% and 1.0%, respectively, with the absolute maximum RDR value of 2.5% under some ground motions. Table 4 summarizes the average values of RDR at various story levels of BRBFs with Chevron as well as Double-X brace configurations. It should be noted that the maximum value of RDR is noted at the first story of BRBFs with the Chevron braces, whereas the same is noted at the fourth story level in case of the Double-X brace configurations. Similar to the ISDR response, no significant difference in the RDR response is noted between the types of beam-to-column connections used in BRBFs. Hence, the BRBFs can exhibit smaller post-earthquake residual drift response under near-fault earthquakes if all BRBs are arranged in Chevron configurations only. It should be noted that in calculating the average values of drift response, the NF23 ground motion has been excluded since all BRBFs collapsed due to the formation plastic hinges reaching their rupture points in beams and columns, thus resulting significantly larger drift values, as discussed in the following section.

5.3 Brace ductility and hinge mechanisms

As expected, the inelastic BRB deformations are noted under each ground motion. Brace ductility demand is computed as the ratio of the maximum axial deformation of BRBs (in tension or compression) to their corresponding yield values under any ground motion. Fig. 8(a) shows the variation of the maximum displacement ductility demand on BRBs of BRBFs. A relatively higher BRB ductility demand is noted for the BRBFs with Double-X brace configurations as compared to those with Chevron configurations under all the selected ground motions. For BRBFs with the Chevron braces, the maximum BRB ductility demand is found to be smaller than the design

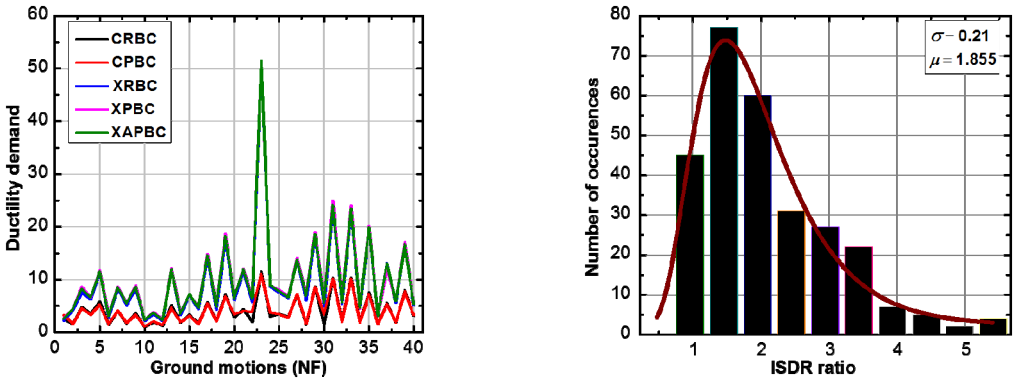

(a) (b)

Fig. 8 (a) BRB displacement ductility response; and (b) variation of ISDR response of CRBC frame

limit of 25 with the absolute maximum ductility value of 11.1 is noted under NF 23 ground motion. In case of BRBFs with Double-X brace configurations, the maximum ductility demand on BRB is found to be 51.4 under the NF 23 ground motion indicating the failure of BRBs. The ductility demand on BRBs also reached the design limit of 25 under the NF 31 and NF 33 ground motions in case of the BRBFs with Double-X brace configuration. However, the ductility demand on BRBs is smaller than the design limit under all other ground motions. The average value of displacement ductility demand on BRBs is noted as 6.8 in case of the Chevron configuration, whereas the corresponding value is found to be 15.3 in case of the Double-X brace configuration. Thus, the excellent displacement ductility characteristics of BRBs in BRBFs are relatively under-utilized in case of the Chevron configurations as compared to that in the Double-X configurations.

Table 5 shows the hinge formations in the beams and columns at various story levels of BRBFs under the selected ground motions. In case of the CRBC frame, yielding (represented by "B") of columns is noted at the ground floor level and no other plastic hinges are noted in the columns at the intermediate story levels. Similarly, the yielding of beams is noted at the lower story levels (up to fourth story levels) of the CRBC frame. Except the NF 23 ground motion, the ultimate strengths of beams and columns are not exceeded in the plastic hinges under the selected ground motions. In case of CPBC frame, the yield of columns is noted at their bases under all ground motions except the NF 07 and NF 23 ground motions, the flexural strength of columns at the ground floor level reached their ultimate values. In case of the BRBFs with Double-X braces, the yielding of beams and columns at the intermediate story levels is noticed in addition to those at the ground floor level. These frame members reached their ultimate flexural strengths under some ground motions. A reduced number of plastic hinges are formed in the beams of BRBF with Double-X braces and alternate RBC connections due to the introduction of moment release at the pinned ends. Since the plastic hinging in columns should be limited to their bases and the plastic hinges should be not allowed to form in the intermediate columns at the mechanism stage for an acceptable structural response, BRBs arranged in the Chevron configurations should be preferred instead of the Double-X BRB configurations in the BRBFs located in the near-fault regions.

6. Fragility analysis

Fig. 8(b) show the plot between the number of occurrence and ISDR response of a BRBF with Chevron brace arrangements under the selected ground motions. The ISDR distribution plot is skewed towards the smaller drift values of amplitude less than 1.5%. The number of occurrence rapidly decreases at the higher drift levels indicating log-normal distribution of ISDR response. A fragility curve represents the probability of reaching or exceeding a damage state at a specified seismic hazard level. Thus, log-normal probability density function has been considered for the fragility analysis in this study in which μ and σ values of the Engineering Demand Parameter (EDP) have been calculated for all the ground motions. The probability of exceedance (p) of each EDP, computed using a cumulative normal distribution function (ϕ), can be expressed as follows

$$p(EDP > x) = 1 - F(\chi) = 1 - \phi\left(\frac{\ln(x) - \mu}{\sigma}\right), \quad x > 0 \tag{1}$$

Where, $F(\chi)$ is the cumulative distribution function (CDF). Since the drift response is used as an indicator of the damages in a structure, the fragility curves are developed for all study frames

considering the ISDR and RDR as the damage parameters. It is worth mentioning that other parameters, such as, Peak ground Acceleration (PGA), Spectral acceleration, etc., have also been used as the EDP by various researchers in the fragility analysis of structures.

Fig. 9(a) shows the probability of exceedance of the absolute peak ISDR response of BRBFs. These peak values are considered as the maximum drift response of BRBFs irrespective of the story levels where they occurred under the selected ground motions. BRBFs with Chevron

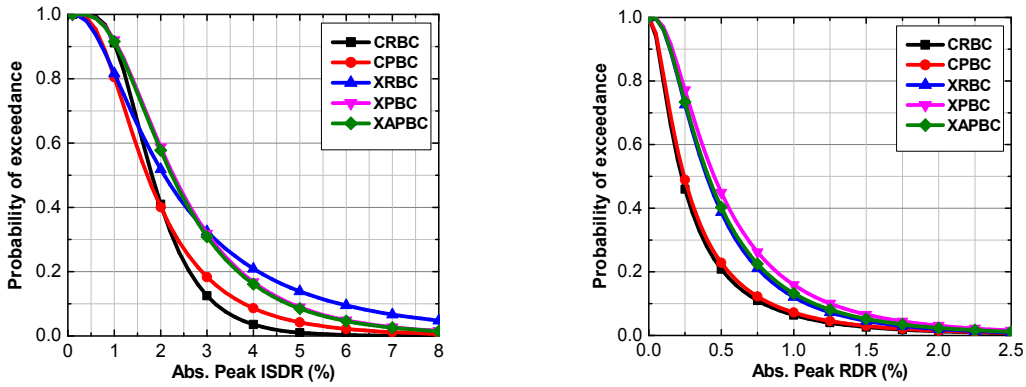

(a) (b)

Fig. 9 Fragility curves of absolute peak: (a) ISDR; and (b) RDR response of BRBFs

Table 5 Details of plastic hinges formed in frame members of BRBFs

Ground motions	CRBC		CPBC	XAPBC		XRBC		XPBC
	Beam	Column	Column	Beam	Column	Beam	Column	Column
NF03	1S1B	1S2B	1S2B	-	-	-	-	-
NF05	1S2B, 2S2B, 3S2B	1S2B	1S2B	2S1B, 4S1B	1S1B	1S2B, 2S1B, 3S2B, 4S1B	1S1B	1S1B, 5S1B
NF07	-	1S2B	1S1B	2S1B, 4S1B	-	1S2B, 2S1B, 4S1B	-	-
NF13	1S2B, 2S2B, 3S2B, 4S1B	1S2B	1S2B	2S1B, 4S1B, 6S1B	-	1S2B, 2S1B, 3S2B, 4S2B, 6S1B	-	5S1B
NF15	-	1S1B	-	-	-	-	-	-
NF17	1S2B, 2S2B, 3S2B, 4S2B, 5S1B	1S2B	1S2B	4S1B, 6S1B	6S1B	2S1B, 3S2B, 4S2B, 5S1B, 6S1B	4S1B, 6S2B	5S1B
NF19	1S2B, 2S2B, 3S1B, 4S1B	1S2B	1S2B	2S2B, 4S2B, 6S1B	1S1B, 2S1B, 6S1B	1S2B, 3S2B, 4S2B, 5S2B, 6S1B	1S1B, 2S1B, 4S1B, 6S2B	1S1B, 3S1B, 5S1B
NF21	1S1B	1S2B	1S2B	2S1B, 4S1B	-	1S1B, 2S1B, 3S1B, 4S1B	-	-

Table 5 Continued

Ground motions	CRBC	CPBC		XAPBC		XRBC		XPBC
	Beam	Column	Column	Beam	Column		Beam	Column
NF23	1S2E, 2S2E, 3S2E, 4S2B, 5S1B1E, 6S2B	1S2E	1S2E	2S1B1E, 4S2E, 6S2B	1S2B1E, 2S2B, 3S1B2E, 4S3B1E, 5S2B1E, 6S2B1E	1S2E, 2S2E, 3S2E, 4S2E, 5S1B1C, 6S2B, 7S2B	1S1B3E, 2S1B3E, 3S4E, 4S1B3E, 5S1B3E, 6S4B, 7S3B	1S2B1E, 2S2B, 3S1B2E, 4S1B1E, 5S2B1E, 6S2B, 7S1B
NF24	-	-	-	-	-	4S1B	-	-
NF27	1S2B, 2S2B	1S2B	1S2B	2S2B, 4S2B, 6S1B	1S2B, 3S1B, 4S1B, 5S1B	1S2B, 2S2B, 3S2B, 4S2B, 6S1B	1S2B, 3S1B, 4S1B, 5S1B	1S2B, 3S1B, 4S1B, 5S1B
NF29	1S2B, 2S2B, 3S2B, 4S1B	1S2B	1S2B	2S2B, 4S2B, 6S1B	1S2B, 3S1B, 5S1B	1S2B, 2S2B, 3S2B, 4S2B, 5S2B, 6S1B	1S2B, 3S1B, 4S1B, 5S1B, 6S1B	1S2B, 3S1B, 5S1B
NF31	1S2B, 2S2B, 3S2B, 4S2B, 5S2B	1S2B	1S2B	2S2B, 4S2B, 6S2B	1S3B, 2S1B, 3S2B, 4S2B, 5S1B, 6S1B	1S2B, 2S2B, 3S2B, 4S2B, 5S2B, 6S2B	1S2B, 2S1B, 3S1B, 4S2B, 5S1B, 6S2B	1S3B, 3S2B, 4S1B, 5S1B
NF33	1S2B, 2S2B, 3S2B, 4S2B, 5S1B	1S2B	1S2B	2S2B, 4S2B, 6S1B	1S3B, 2S1B, 3S2B, 4S2B, 5S1B, 6S1B	1S2B, 2S2B, 3S2B, 4S2B, 5S2B, 6S1B	1S2B, 2S1B, 3S1B, 4S2B, 5S1B, 6S2B	1S2B, 3S2B, 4S1B, 5S1B
NF35	1S2B, 2S2B, 3S2B, 4S2B	1S2B	1S2B	2S2B, 4S2B, 6S1B	1S3B, 2S1B, 3S2B, 4S2B, 5S1B, 6S1B	1S2B, 2S2B, 3S2B, 4S2B, 5S2B, 6S1B	1S2B, 2S1B, 3S1B, 4S2B, 5S1B, 6S2B	1S2B, 3S2B, 4S1B, 5S1B
NF37	1S2B	1S2B	1S2B	2S1B, 4S1B, 6S1B	1S1B	1S2B, 2S2B, 3S2B, 4S2B, 6S1B	1S2B	1S1B, 5S1B
NF39	1S2B, 2S2B, 3S2B, 4S2B	1S2B	1S2B	2S2B, 4S2B, 6S1B	1S2B, 3S1B, 5S1B	1S2B, 2S2B, 3S2B, 4S2B, 5S2B, 6S1B	1S2B, 3S1B, 4S1B, 5S1B, 6S1B	1S2B, 3S1B, 4S1B, 5S1B

*Note: *mSnX* stands for "*n*" number of hinges at story "*m*" with hinge status as "X".
Hinge status can be Yield (B), or Ultimate (C), or Rupture (E)

brace configurations exhibited nearly similar fragility curves for both RBC and PBC connections. In both cases, the probability of exceeding the peak ISDR value of 2% is noticed as 40% for BRBFs with Chevron brace configurations. However, BRBFs with PBC connections exhibited marginally higher probability of exceedance for the peak ISDR values greater than 2% as compared to those with the RBC connections. BRBFs with Double-X brace configurations exhibited the higher probability of exceedance of peak ISDR values at the higher drift levels for all combination of beam-to-column connections as compared to those with Chevron configurations. For example, the probability of exceedance for the peak ISDR value of 2% is noted as nearly 60% for Double-X configurations as compared to 40% for Chevron configurations. However, XRBC

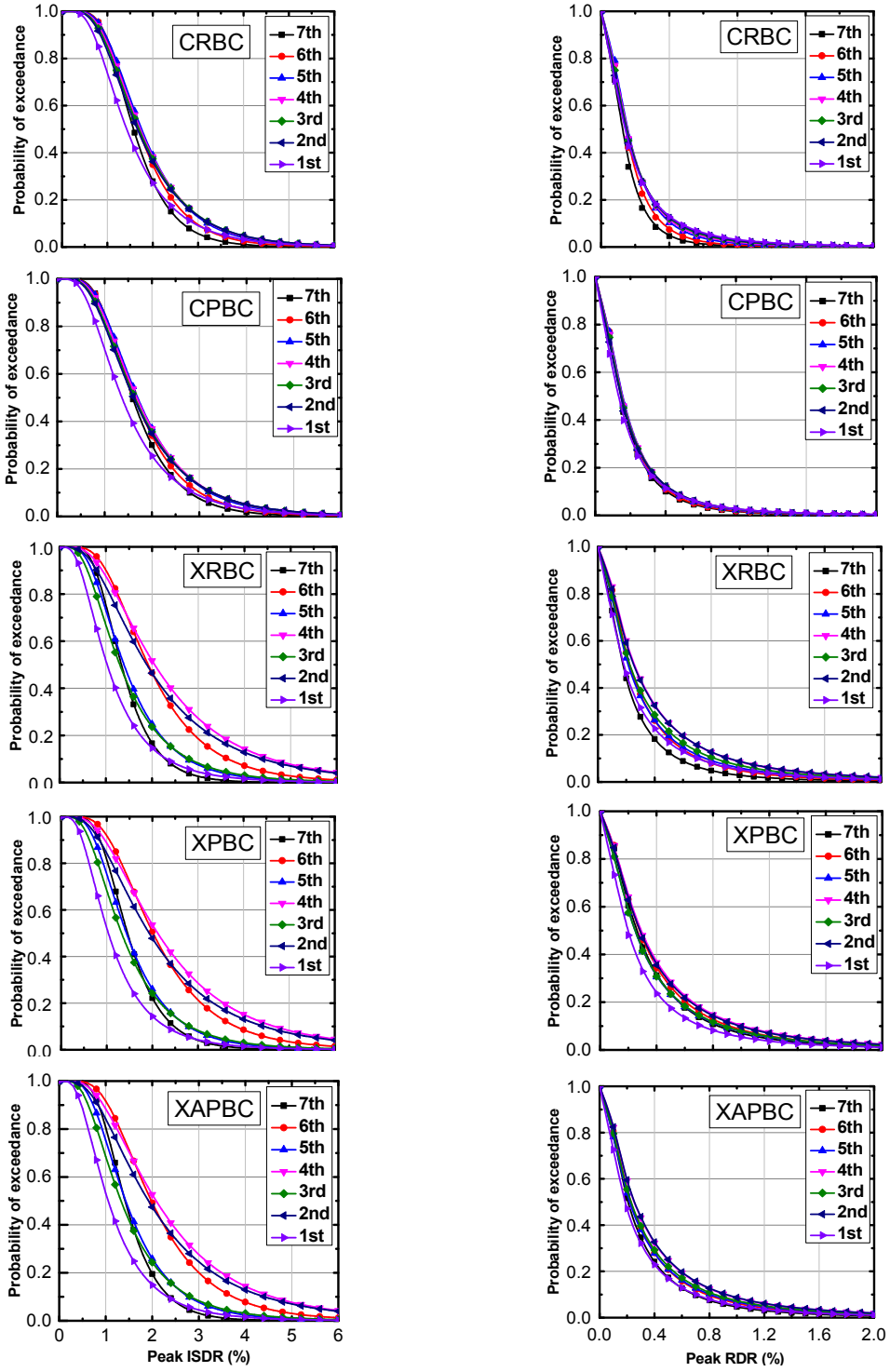

Fig. 10 Fragility curves of peak: (a) ISDR; and (b) RDR response at various story levels of BRBFs

frame exhibited a higher probability of exceedance of peak ISDR value greater than 3%. This may be due to the formation of a relatively higher number of plastic hinges in beams and columns because of moment-resisting connections (Table 5). As shown in Fig. 9(b), both CRBC and CPBC frames exhibited nearly same probability of exceedance for the peak RDR values less than 2.5%. Similar to the ISDR response, BRBFs with Double-X brace configurations exhibited the higher probability of exceedance for the peak RDR response as compared to those with Chevron configurations.

Fig. 10(a) shows the comparison of ISDR response at various story levels of BRBFs. The probability of exceedance for the peak ISDR response of BRBFs with Chevron brace configurations is relatively smaller at the first story level up to a drift level of about 2%, beyond which the smaller probability of exceedance of ISDR is noted at the seventh story level as compared to all other stories. No significant difference is noted in the ISDR response at the intermediate story levels of BRBFs with Chevron configurations. In case of BRBFs with Double-X brace configurations, a relatively higher value of probability of exceedance of ISDR response is noted at the story levels where the BRBs are connected to the beams as compared to all other stories. The probability of exceedance of the peak ISDR value of 2% is found to be 50% at the story levels where braces do not intercept the beams of BRBFs with Double-X brace configurations, whereas the corresponding value of probability of exceedance for the BRBFs with Chevron configurations is noted as 25%. As shown in Fig. 10(b), the probability of exceedance of the peak RDR response is nearly same at all the story levels of BRBFs with both Chevron and Double-X brace configurations. Further, BRBFs with Double-X brace configurations exhibited the higher probability of exceedance of the peak RDR as compared to those with Chevron configurations.

The plastic hinge mechanism and the drift response of BRBFs under near-fault ground motions as presented in this study are nearly similar to those for far-field earthquakes as reported by Ghowsi and Sahoo (2010). In general, the higher drift response is noted for the Double-X brace configurations as compared to the Chevron configurations. This is primarily due to the formation of plastic hinges in the columns at the intermediate story levels of BRBFs with Double-X brace configurations (Table 5). In case of BRBFs with BRBs arranged in Chevron configurations, the plastic hinges are formed at the first story column bases in most of the selected ground motions. In addition, in case of RBC connections, a relatively large number of plastic hinges are formed in the beams of Double-X configurations as compared to the Chevron configurations. This also resulted a relatively smaller residual drift response for BRBFs with Chevron configurations as compared to the Double-X configurations.

7. Conclusions

Based on the analysis results, following conclusions can be drawn for the medium-rise BRBFs:

- The average value of interstory drift response of BRBFs with Double-X brace configurations exceeded the drift limit of 2% at the story levels where the braces do not intercept the beams. However, the average values of interstory drift response for BRBFs with the Chevron BRB configurations are less than this drift limit for either rigid or pinned beam-to-column connections. BRBFs exhibited the smaller post-earthquake residual drift response under the near-fault ground motions if all BRBs are arranged in the Chevron configurations.

- The maximum displacement ductility characteristics of BRBs can be efficiently utilized in Double-X brace configurations as compared to Chevron configurations in BRBFs located in the near-fault regions. The average value of displacement ductility demand on BRBs is noted as 6.8 in case of the Chevron configurations as compared to a value of 15.3 for the Double-X configurations.
- BRBFs with the Double-X brace configurations exhibit the higher interstory drift and residual drift response under near-fault ground motions. This is primarily due to the formation of plastic hinges in the columns and beams at the intermediate story levels. However, the plastic hinges in columns of BRBFs with Chevron configurations are mostly formed at the first story level only.
- The probability of exceedance of residual drift response is nearly same at all the story levels for the BRBFs with either Chevron or Double-X brace configurations. BRBFs with pinned beam-to-column connections exhibit marginally higher residual drift response under the near-fault ground motions as compared to the rigid beam-to-column connections.

References

Aiken, I.D., Mahin, S.A. and Uriz, P.R. (2002), "Large-scale testing of buckling-restrained braced frames", *Proceedings of Japan Passive Control Symposium*, Tokyo Institute of Technology, Japan.

ANSI/AISC 341-05 (2005), Seismic Provisions for Structural Steel Buildings; American Institute of Steel Construction, Chicago, IL, USA.

ASCE/SEI 7-10 (2010), Minimum Design Loads for Buildings and other Structures; American Society of Civil Engineers, VA, USA.

Avci-Karatas, C., Cetinkaya, S., Demir, C., Comert, M., Gunes, B. and Celik, O.C. (2013), "Cyclic testing of a steel-core buckling restrained brace (BRB) under near-fault displacement reversals", *Proceedings of the 2nd Conference on Smart Monitoring*, *Assessment and Rehabilitation of Civil Structures* (*SMAR*' *2013*), Istanbul, Turkey, September.

Baghbanijavid, Z., Jalali, A. and Yasrebinia, Y. (2010), "Seismic response of buckling-restrained braced frames under near fault ground motions", *J. Appl. Sci.*, **10**(23), 2967-2977.

Black, C.J., Makris, N. and Aiken, I.D. (2004), "Component testing, seismic evaluation and characterization of buckling-restrained braces", *ASCE J. Struct. Eng.*, **130**(6), 880-894.

Chou, C.C., Liu, J.H. and Pham, D.H. (2012), "Steel buckling-restrained braced frames with single and dual corner gusset connections: seismic tests and analyses", *Earthq. Eng. Struct. Dyn.*, **41**(7), 1137-1156.

CSI (2009), CSI Analysis Reference Manual for SAP 2000; Computers and Structures, Inc., Berkeley, CA, USA.

Fahnestock, L.A., Sause, R. and Ricles, J.M. (2007), "Seismic response and performance of buckling-restrained braced frames", *ASCE J. Struct. Eng.*, **133**(9), 1195-1204.

FEMA 356 (2000), Prestandard and Commentary for the Seismic Rehabilitation of Buildings; Federal Emergency Management Agency, Washington, D.C., USA.

FEMA 450 (2003), NEHRP Recommended Provisions for Seismic Regulations for New buildings and Other Structures; Part 1- Provisions, Federal Emergency Management Agency, Washington, D.C., USA.

Field, C. and Ko, E. (2004), "Connection performance of buckling-restrained braced frames", Paper No. 1321, *Proceedings of the 13th World Conference on Earthquake Engineering*, Vancouver, BC, Canada, August.

Ghowsi, A.F. and Sahoo, D.R. (2013), "Seismic performance of buckling-restrained braced frames with varying beam-column connections", *Int. J. Steel Struct.*, **13**(4), 607-621.

Huang, Y.C. and Tsai, K.C. (2002), *Experimental Responses of Large Scale Buckling Restrained Brace Frames*, Report no. CEER/R91-03; National Taiwan University, Taiwan. [In Chinese]

Iwata, M., Kato, T. and Wada, A. (2003), "Performance evaluation of buckling-restrained braces in damage-controlled structures: Behavior of steel structures in seismic area", *Proceedings of the 4th International Conference STESSA*, Naples, Italy, June.

Lin, M.L., Tsai, K.C., Hsiao, P.C. and Tsait, C.Y. (2005), "Compressive behavior of buckling restrained braces gusset connections", *Proceedings of the 1st International Conference on Advances in Experimental Structural Engineering*, Nagoya, Japan, July.

López, W.A. and Sabelli, R. (2004), *Seismic Design of Buckling-Restrained Braced Frames*, Structural Steel Education Council, Moraga, CA, USA.

Merritt, S., Uang, C.M. and Benzoni, G. (2003), *Subassemblage Testing of Core Brace Buckling-Restrained Braces*, Report No. TR-2003/01; Department of Structural Engineering, University of California at San Diego, CA, USA.

Romero, P., Revelry, L., Miller, P. and Okahashi, T. (2003), *Full-Scale Testing of WC Series Buckling-Restrained Braces*, Deptartment of Civil and Environmental Engineering, University of Utah, UT, USA.

Sahoo, D.R. and Chao, S.-H. (2010), "Performance-based plastic design method for buckling-restrained braced frames", *Eng. Struct.*, **32**(9), 2950-2958.

SEAOC (1999), Seismic Design Manual. Vol. I - Code Application Examples; Structural Engineers Association of California, Sacramento, CA, USA.

Shakib, H. and Safi, R. (2012), "Behavior evaluation of the eccentric buckling-restrained braced frames under the near-fault ground motions", *Proceedings of the 15th World Conference of Earthquake Engineerng*, Lisbon, Portugal, September.

Somerville, P.G., Smith, M., Punyamurthula, S. and Sun, J. (1997), Development of ground motion time histories for phase 2 of the FEMA/SAC Steel Project, Report No. SAC/BD-97/04; SAC Joint Venture, Sacramento, CA, USA.

Tsai, K.C., Hsiaso, B.C., Lai, J.W., Chen, C.H., Lin, M.L. and Weng, Y.T. (2003a), "Pseudo-dynamic experimental response of a full-scale CFT-BRB composite frame", *Proceedings of Joint NCREE/JRC Workshop on International Collaboration on Earthquake Disaster Mitigation Research*, Taipei, Taiwan, November.

Tsai, K.C., Loh, C.H., Hwang, Y.C. and Weng, C.S. (2003b), "Seismic retrofit of building structures with dampers in Taiwan", *Proceedings of Symposium on Seismic Retrofit of Buildings and Bridges with Base Isolation and Dampers*, Kyoto, Japan, January.

Usami, T., Kasai, A. and Kato, M. (2003), "Behavior of buckling-restrained brace members: Behavior of Steel Structures in Seismic Areas", *Proceedings of the 4th International Specialty Conference STESSA*, Naples, Italy, June.

Watanabe, A., Hitomi, Y., Saeki, E., Wada, A. and Fujimoto, M. (1988), "Properties of brace encased in buckling-restrained concrete and steel tube", *Proceedings of the 9th World Conference on Earthquake Engineering*, Tokyo, Japan, August.

CC